MODELING ECRIS PLASMA USING 2D GEM* (GENERAL ECRIS MODEL)

L. Zhao#, J. S. Kim, B. Cluggish,
FAR-TECH, Inc., San Diego, CA 92121, U.S.A.

Abstract

The GEM 1D code [1] is developed by FAR-TECH, Inc. to model the plasmas in ECRIS devices using experimental knobs such as the magnetic field, rf power and frequency, and the geometry of the device. The code models EDF (electron distribution function) by solving Fokker-Planck equation, ions as fluid and neutrals by particle balancing. It has been extended to include 2D (axial and radial) spatial features such as 2D ECR heating and ion radial diffusion. The convergence and consistency of the code have been studied. It is parallelized using the MPI technique to boost the calculation speed. Results of the GEM 2D simulation and comparisons of GEM 2D with GEM 1D results and experimental measurements will be presented. The predicted hollow profile of ECRIS plasma is consistent with experimental observations.

INTRODUCTION

GEM 2D is extended from an advanced ECRIS modeling code, GEM 1D, which has been developed by FAR-TECH to predict axial steady-state ECRIS plasma profiles and charge state distribution (CSD) of output beam self-consistently using experimental knobs as input, such as rf power, rf frequency, gas pressure, and device configurations. GEM 1D calculates non-Maxwellian EDF (electron distribution function) of hot electrons using a bounce-averaged Fokker-Planck code [2] and solves the flow of the cold ions using 1D ion fluid code. It has obtained some numerical results consistent with experiments. However, the further applications of GEM to beam capture [3] and beam extraction simulation require GEM to be extended to 2D to acquire both axial and radial profiles of the plasma parameters. Also, 2D models can simulate the complicate magnetic field in ECRIS and ECR heating zone more accurately. This paper presents the modeling theories of GEM 2D and the results of the simulation of a typical ECRIS device, ECR-I in ANL [4]. The comparisons with GEM 1D results and experimental data will also be presented and discussed.

DESCRIPTION OF GEM 2D MODELS

GEM-1D simulates the dynamics of an ECRIS plasma along the field lines but assumes the plasma is uniform in the radial direction. GEM 2D is extended from GEM 1D by adding a radial dimension to GEM 1D's numerical models. It can predict ECRIS plasma in both radial and axial directions by a combination of 2D physical models including 2D magnetic field and ECR heating modeling, bounce-averaged Fokker-Planck EDF modeling and 2D ion fluid modeling. In the following discussion, we will use ECR-I at ANL as the standard device for the simulation. The typical operation parameters are listed in table 1.

Table 1: Operating parameters for ECR-I

Parameters	Typical Values
Plasma	Oxygen
Length	29 cm
Radius	4 cm
Gas pressure	1.2e-7 Torr
rf power	323W
rf frequency	10 GHz
B field ratio	4.5 and 3

2D modeling of the Magnetic field and ECR resonance surface

The magnetic field on ECR-I is a typical minimum-B structure which is composed by a mirror field and a hexapole field. The full 3D ECR resonance surface is a football shape structure [5] which depends on z, r, θ in cylindrical coordinate. For 2D simulations, the magnetic field is azimuthally averaged to eliminate θ dependence. The radial grids are tied onto the flux surfaces that are evenly distributed on the mid-plane and then extended to the whole chamber along the field lines (Fig 1a). The axial profiles of the field strength on the field flux surfaces are plotted in Fig. 1b. Note that the field strength increases with radius. This is because while we average over the hexapole variation in the direction of magnetic field, the magnitude of the hexapole field strength is still included in GEM-2D. This allows a proper calculation of the ECR resonance zone.

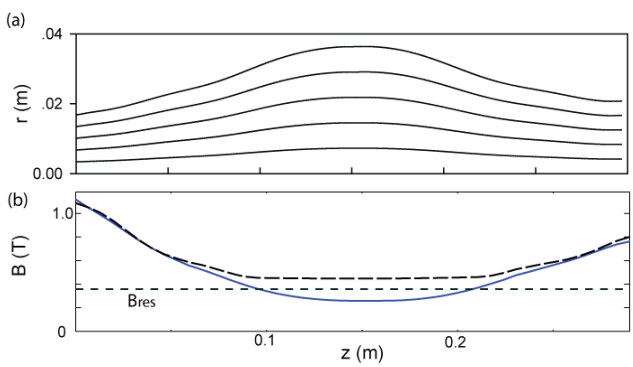

Figure 1: a) Radial grids that are tied onto the magnetic

field lines. b) Magnetic field strengths along the field lines. The short dashed line is the resonance field, B_{res} =0.357 T. The solid line is the field along the field line that is at r=0, the long dashed line is the field along the field line outside of the resonance zone at r=0.03m.

The 2D azimuthally averaged ECR resonance surface is shown in Fig. 2. The ECR resonance surface is a closed surface which is distributed on both radial and axial directions. GEM 2D can model the ECR heating surface with fairly good accuracy compared with the full 3D ECR resonance surface while GEM 1D has to ignore the radial dependence of ECR heating. The radial dependence of the later GEM 2D results is mainly from this 2D feature of the ECR heating.

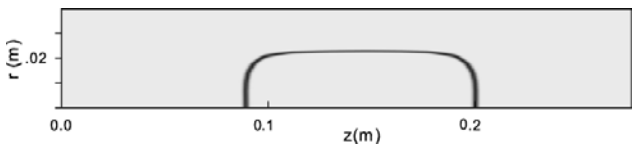

Figure 2: Azimuthally averaged ECR resonance surface modeled by GEM 2D.

Fokker-Planck Electron modeling

In a typical ECR plasma, electrons are hot (temperature >1 keV) due to ECR heating and the electron collision frequency is much less than the bounce frequency in the mirror field. As a result, the electron distribution function (EDF) is usually highly non-Maxwellian (Fig 3).

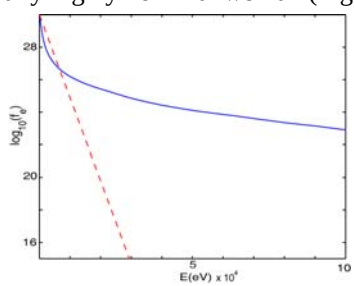

Figure 3: An example of non-Maxwellian EDF of ECRIS plasma modeled by GEM (solid line) and a Maxwellian EDF (dashed line), which drops exponentially with electron energy.

A bounce-averaged Fokker-Planck code [4] is feasible for predicting EDF on the midplane, $f(\upsilon,\theta_\upsilon;z_{mid})$, for mirror confined plasmas. The plasma parameters are averaged over the bouncing orbits in the mirror field under the assumption that the bouncing frequency is much greater than the collision frequency. EDF is then mapped axially along the magnetic flux surface through electron energy conservation and magnetic momentum conservation. Since the radial transport of electrons is negligible, EDF on each radial grid can be calculated independently using the same technique. The obtained full EDF $f(\upsilon,\theta_\upsilon;z,r)$ is then used in the ionization calculations and ion fluid modeling.

The ECR heating term is treated using the same bounce-averaging technique as the collision term in the Fokker-Planck code. The ECR power deposited in the plasma is described by four velocity space diffusion coefficients which are proportional to the rf power and have the 2D spatial profile shown in Fig 2.

2D fluid ion modeling

Since the ions in ECRIS plasma are highly collisional and cold (only ~1eV), the ions are treated as fluid. The 2D ion continuity equation for ions of species *j* and charge state *q* is

$$\frac{\partial n_{j,q}}{\partial t}+\frac{1}{A_z}\frac{\partial}{\partial z}\left[A_z n_{j,q}u_z\right]+\frac{1}{r}\frac{\partial}{\partial r}\left[r n_{j,q}u_{r\,j,q}\right]=S_{j,q} \quad , \quad (1)$$

where A_z is grid cross-section, u_z and u_r are ion velocity in axial and radial direction, S is a source/sink term that includes gains and/or losses due to ionization and charge-exchange. The axial velocity u_z is assuming to be the same for different ion species, but the radial velocity u_r is different due to the difference in Coulomb collision rates. The radial velocity u_r in Eq. 1 can be calculated by radial and azimuthal momentum equations,

$$m_j n_{j,q}\frac{\partial u_{j,qr}}{\partial t}=qn_{j,q}e(E_r+u_{j,q\theta}B)-k_B T_{j,q}\frac{\partial n_{j,q}}{\partial r}-F_r^{jk}$$

$$F_r^{jk}=n_{j,q}\sum_{k,p}\mu_{jk}n_{k,p}K_{j,q\to k,p}(u_{j,qr}-u_{k,pr})$$

$$m_j n_{j,q}\frac{\partial u_{j,q\theta}}{\partial t}=-qn_{j,q}eu_{j,qr}B-F_\theta^{jk}$$

$$F_\theta^{jk}=n_{j,q}\sum_{k,p}\mu_{jk}n_{k,p}K_{j,q\to k,p}(u_{j,q\theta}-u_{k,p\theta}) \quad (2)$$

E and B are electrical and magnetic field in the plasma, F is the friction force due to ion-ion Coulomb collisions, μ is the collision rate. The convection term is ignored since the velocities are slow.

The ion momentum equation in axial direction is

$$n_e\frac{\partial u_i}{\partial t}=-\frac{J_r}{e}\frac{\partial u_i}{\partial r}-n_e u_i\frac{\partial u_i}{\partial z}-\sum_{j,q}\frac{qk_B T_{j,q}}{m_j}\frac{\partial n_{j,q}}{\partial z}+$$

$$\sum_{j,q}qS_{j,q}^{in}\left(\langle u\rangle^{in}-u_i\right)+E_z\sum_{j,q}\frac{qn_{j,q}e}{m_j} \quad (3)$$

The axial electrical field E_z and plasma potential (the integral of E) can be solved from this equation together with the electron continuity equation.

RESULTS AND DISCUSSION

The GEM 2D has successfully simulated the plasma in ECR-I with typical parameters listed in Table 1. For this particular run, the radial grid number was set as 12. The calculation was parallelized on 6 processors using MPI technique.

Figure 4 shows the 2D potential profile in the plasma. The potential profile shows a “dip” in the center of the plasma, as has been previously predicted. This dip confines the ions in both the axial and radial directions.

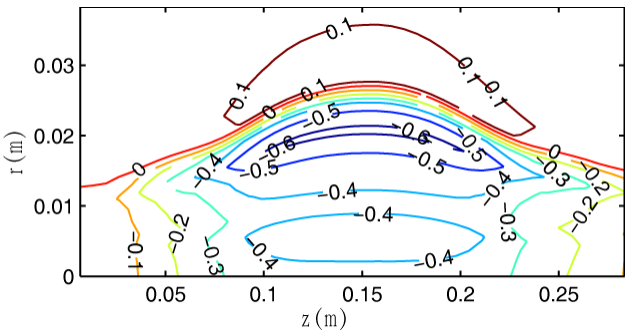

Figure 4: The contour plot of the plasma potential modeled by GEM 2D. Potential is in volts.

The profiles of electron density, temperature, ion density and ion fluxes that are predicted by GEM 2D modeling are showing clear radial dependence due to the spatial distribution of ECR heating in Fig. 2. For example, the predicted electron density profile shown in Fig 5 is a hollow profile with the density peaked at the ECR resonance surface which is 2 cm away from the device center. The hollow profile of ECRIS plasma has also been observed in the experiments [6,7]. GEM simulation results and the experimental results are showing that the plasma density peaks around the ECR heating surface. Also, the GEM 2D result is matched well with the profile predicted by GEM 1D (Fig. 5b), which predicts the radially averaged ECR plasma by assuming that the ECR heating profile has no radial dependence.

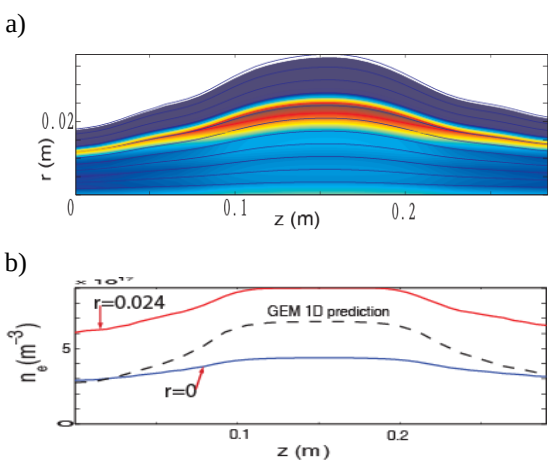

Figure 5: a) The contour plot of the plasma density modeled by GEM 2D. b) The axial profiles of the plasma density at different radial positions and the comparison with GEM 1D prediction (dashed line).

The extracted ion charge state distribution (CSD) has shown similar radial dependence as the plasma density profile. To compare with GEM 1D result and the experimental data discussed in [1], CSD calculated by GEM 2D is obtained by integrating the ion extraction current density over the cross-sections along the radial direction (Fig. 6). The CSD predicted by GEM 2D is more consistent with the experimental data than GEM 1D predictions.

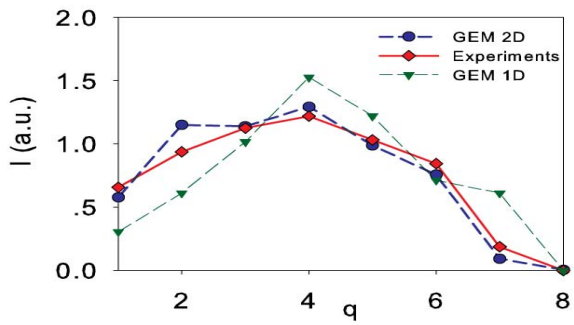

Figure 6: CSD predicted by GEM 2D (dots), GEM 1D (triangles) and experimental measurements (diamonds).

CONCLUSIONS

Extended from GEM 1D, GEM 2D is an advanced ECRIS plasma modeling tool which can simulate ECRIS plasma in both radial and axial directions. GEM 2D calculates 2d2v non-Maxwellian EDF $f(\upsilon,\theta;z,r)$ of the electrons by solving Fokker-Planck equation using bounce-averaging method and the spatial transport of cold ions by solving 2D fluid equations. The results of GEM 2D simulation of ANL ECR-I are consistent with the experimental data and observations.

Future work of GEM 2D will be focused on the validation of GEM 2D using available experimental data and the application of the GEM 2D on charge-breeder optimizations and ion extraction studies.

REFERENCES

[1] D.H. Edgell, J.S. Kim, and I.N. Bogatu, R.C. Pardo and R.C. Vondrasek, Rev. Sci. Instrum., **73**, 641 (2002).

[2] A. Mirin, M. McCoy, G. Tomaschke and J. Killeen, *Comput. Phys. Commun.* **81**, 403 (1994)

[3] J.S. Kim, C. Liu, D.H. Edgell, and R. Pardo, *Rev. Sci. Instrum.*, **77**, 03B106 (2006).

[4] F. Ames, R. Baartman, P. Bricault, K. Jayamanna, M. McDonald, M. Olivo, P. Schmor, D.H.L. Yuan, and T. Lamy, *Rev. Sci. Instrum.*, **77**, 3B103 (2006).

[5] L. Zhao, J. S. Kim, B. Cluggish, "2D Extension of GEM", Proceedings PAC07, Albuquerque NM (2007) .

[6] S. Biri, A. Valek,, and T. Suta, *Rev. Sci. Instrum.*, **75**, 1420 (2004).
[7] P. Grübling, J. Hollandt, and G. Ulm, *Rev. Sci. Instrum.*, **73**, 614 (2002).